Chapter 4: DNA-Mediated Electrochemistry of Disulfides on Graphite

Adapted from: Gorodetsky, A. A., Barton, J. K. (2006) *J. Am. Chem. Soc. 129*, 6074–6075.

ABSTRACT

The electrochemistry of disulfides incorporated into the sugar-phosphate backbone of pyrene-modified DNA has been examined on highly oriented pyrolytic graphite (HOPG). Two signals, one irreversible, one reversible, are observed at -160 and -290 mV versus normal hydrogen electrode, respectively. The inclusion of a single base mismatch in the DNA duplex below the location of the disulfide leads to a significant attenuation in the electrochemical signal, while the inclusion of a mismatch above the disulfide has little effect on the electrochemistry observed. Thus disulfide reduction in the DNA backbone appears to be DNA-mediated. The redox couples found show a strong pH dependence consistent with formation of a disulfide radical anion or 2e- reduction of the disulfide to the two thiols. These data demonstrate that DNA electrochemistry can be utilized to promote disulfide reduction at a distance mediated by the DNA duplex.

4.1 Introduction

The DNA base pair stack has been shown to mediate charge transport over significant distances (1, 2) using a variety of experiments (3–5). Both in solution and at DNA-modified surfaces, DNA-mediated charge transport (CT) chemistry exhibits exquisite sensitivity to perturbations of the intervening base pair stack such as single base mismatches (6), bulges (7, 8), and protein binding (9–11). However, the mechanisms underlying this chemistry remain poorly understood (12–16). Nonetheless, an overwhelming body of evidence indicates that DNA charge transport provides an efficient route to carry out both oxidative and reductive reactions at a distance (3–8, 17–22).

We have reported that DNA CT can lead to oxidation of thiols incorporated into a DNA duplex with concomitant disulfide bond formation in solution (23). Although the reaction proceeded on the DNA backbone, rather than within the base pair stack, DNA CT was dramatically affected by the inclusion of both proximal and distal single base mismatches. These findings indicated that oxidation of thiols did, in fact, occur *via* the base pair stack. Furthermore, these findings were particularly significant given the importance of thiol chemistry *in vivo*.

Electrochemistry at DNA-modified gold surfaces has been utilized in the development of new methodologies for mismatch detection (24, 25) and in probing DNA-protein interactions (26). These investigations rely on reductive DNA CT chemistry and have frequently made use of DNA-bound, redox active substrates whose electrochemistry is exquisitely sensitive to the integrity of the base pair stack. In

particular, mechanistic studies of CT at DNA-modified surfaces have greatly benefited from the use of probes which are covalently attached to the DNA (27–29).

Recently, DNA-modified highly oriented pyrolytic graphite (HOPG) has been developed as an attractive alternative to gold (30). DNA monolayers on HOPG have been extensively characterized via electrochemistry, AFM, and radioactive labeling. As on gold, dense monolayers with surface densities of ~ 40 pmol/cm^2 are assembled in the presence of Mg^{2+} on graphite. Relative to gold, graphite is certainly better suited for exploring the electrochemistry of disulfide bond formation, which would be complicated by the ease of S-Au bond formation (31). Therefore, this work explores the reversible electrochemical reduction of disulfides covalently incorporated within the sugar-phosphate backbone at self-assembled DNA monolayers on HOPG.

4.2 Experimental Section

4.2.1 Materials

All reagents for DNA synthesis were purchased from Glen Research. Reagents used in the synthesis of pyrene- and thiol-modified DNA were purchased from Sigma in the highest purity available and used as received. SPI-1 HOPG was purchased from SPI, Inc. Buffers were prepared with Milli-Q water and filtered with a 0.2 μm filter.

4.2.2 General Oligonucleotide Synthesis

Oligonucleotides were prepared using standard phosphoramidite chemistry on an ABI 392 DNA Synthesizer. DNA was purified by HPLC on a reverse phase C18 column with acetonitrile and ammonium acetate as the eluents. Unless otherwise noted, all

oligonucleotides were cleaved from the resin with concentrated ammonium hydroxide (NH_4OH) prior to purification. The desired products were characterized by UV-visible spectroscopy and MALDI-TOF mass spectrometry.

4.2.3 Synthesis of 5'-Pyrene-Modified Oligonucleotides

DNA was modified with pyrene at the 5' terminus by following a previously reported procedure (30). In brief, oligonucleotides were prepared by solid-phase synthesis with an unprotected hydroxyl group at the 5' terminus. The 5'-OH was treated with a 120 mg/mL solution of carbonyldiimidazole in dioxane for 2 h followed by an 80 mg/mL solution of 1,6-diaminohexane for 30 min. Subsequently, the free amine was treated with 1-pyrenebutyric acid, *N*-hydroxysuccinimide ester, resulting in the desired pyrene moiety linked to the 5' terminus.

4.2.4 Synthesis of 5'-Thiol-Modified Oligonucleotides

The synthesis of DNA featuring a thiol at the 5' terminus followed previously established procedures (32). In brief, oligonucleotides were prepared by solid-phase synthesis with the commercially available C6 S-S linker phosphoramidite incorporated at the 5' terminus. After deprotection and an initial round of HPLC purification, dithiothreitol was utilized to reduce the disulfide, leaving a free thiol at the 5' terminus. The thiol terminated oligonucleotides were then purified by a second round of HPLC.

4.2.5 Synthesis of 3'-Thiol-Modified and 5'-Pyrene-Modified Oligonucleotides

The synthesis of DNA featuring a thiol at the 5' terminus followed previously established procedures (32). In brief, oligonucleotides were prepared by solid-phase synthesis by utilizing the commercially available 3' C3 thiol modifier S-S CPG. The 3' thiolated sequence was further modified with pyrene at its 5' end as described above.

After deprotection and an initial round of HPLC purification, dithiothreitol was utilized to reduce the disulfide, leaving a free thiol at the 3' terminus and a pyrene moiety at the 5' terminus. The thiol-terminated oligonucleotides were then purified by a second round of HPLC.

4.2.6 Preparation of Duplex DNA

DNA oligonucleotides were suspended in a pH 7.1 buffer containing 5 mM P_i and 50 mM NaCl and quantified via UV-visible spectroscopy. Duplex DNA was then prepared by combining equimolar amounts of both thiolated strands with a complementary 24-mer strand. In the presence of oxygen, the DNA was hybridized by heating equimolar amounts of the three strands to 90 º C, followed by cooling to ambient temperature. In an aerobic buffer for duplex DNA, a disulfide bond is formed between two contiguous thiols incorporated within the DNA backbone in quantitative yields. The reaction is templated by the complementary strand and occurs in negligible yields for the two single strands alone (23).

4.2.7 Melting Temperatures

Melting temperatures (T_m) of all the duplexes were measured using a Beckman DU 7400 spectrophotometer with a temperature control attachment. Absorption at 260 nm of equimolar DNA complements was measured every 1 ºC from 90 to 15 ºC with rate 1 ºC/min. The reverse temperature traces were measured under the same conditions to confirm the reversibility of the DNA annealing process.

4.2.8 Preparation of DNA-Modified Electrodes

DNA modified surfaces were prepared as previously described (30). Briefly, the HOPG surface was cleaned with 3-M scotch tape before each experiment and mounted in

the electrode housing. Duplex DNA containing a pyrene moiety was deposited onto the HOPG surface in buffer, pH 7.1, containing 5 mM P_i 50 mM NaCl, and 100 mM $MgCl_2$; Mg^{2+} is included to ensure a closely packed film. DNA films were allowed to form in a humidified chamber over a period of 24–48 hours.

4.2.9 Electrochemical Experiments

Cyclic and square wave voltammetry experiments were performed using a CH Instruments electrochemical analyzer (Austin, TX). Unless otherwise noted, experiments were performed at ambient temperature in buffer, pH 7.1, containing 5 mM P_i and 50 mM NaCl under an argon atmosphere. A custom-built three-compartment electrochemical cell was used for all experiments with a Pt auxiliary electrode, an SPI-1 grade HOPG working electrode, and a saturated calomel (SCE) reference electrode.

4.2.10 X-Ray Photoelectron Spectroscopy Experiments

Pyrene-modified duplexes were self-assembled on a clean HOPG surface and subsequently dried. XPS data were acquired using an M-Probe X-ray photoelectron spectrometer operated under ultrahigh vacuum (UHV) at 10^{-9}–10^{-8} Torr, as previously described (33).

4.3 Results and Discussion

4.3.1 Surface Characterization by X-Ray Photoelectron Spectroscopy

A DNA modified graphite surface is schematically illustrated in Figure 4.1. Previous AFM characterization found that DNA monolayers on graphite are smooth and featureless with the DNA oriented at a ~ 45 º angle with respect to the surface. For proper

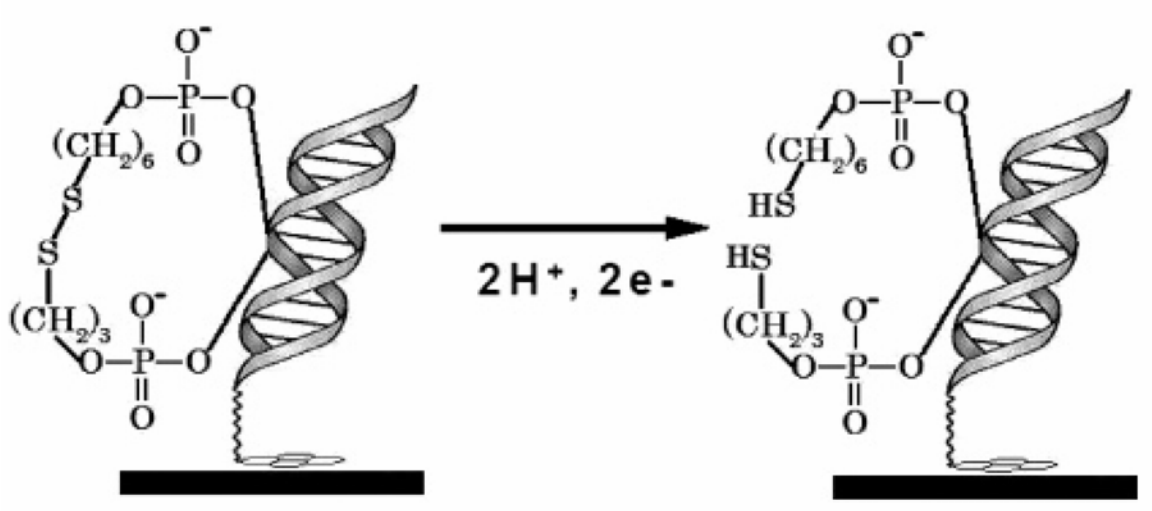

Figure 4.1: Schematic illustration of charge transfer to thiols incorporated into the DNA backbone

interpretation of electrochemical data, some surface characterization is a prerequisite, so the presence of thiols within the DNA monolayer was confirmed here by X-ray photoelectron spectroscopy (XPS) measurements.

DNA monolayers featuring thiols incorporated into the sugar-phosphate backbone reveal a broad S_{2p} peak centered at 164 eV (Figure 4.2). The signal observed is fully consistent with previous XPS measurements of polymer films on gold featuring bound thiols (31, 34). In addition, no signal is observed at a surface modified with DNA which features no backbone modifications. These data provide supporting evidence for the presence of disulfides within the DNA film on graphite.

4.3.2 Thermal Stability of Thiol Modified Duplexes

To further characterize the DNA assembly utilized for subsequent electrochemistry experiments, thermal denaturation experiments were performed. Figure 4.3 shows the sequence and melting temperature of pyrene-modified DNA duplexes featuring no thiols (red), a disulfide (black), only a 3' thiol (light blue), a CA mismatch above the disulfide (dark blue), and a CA mismatch below the disulfide (gray). Well-matched DNA with no thiols has a melting temperature of ~ 70 ºC, and when two thiols are included within the backbone, the duplex is destabilized to a melting temperature of ~ 60 ºC. The incorporation of a CA mismatch, regardless of location, further lowers the melting temperature by another ~ 10 ºC relative to well-matched DNA containing a disulfide (from ~ 60 ºC to ~ 50 ºC).

Interestingly, the incorporation of a solitary 3' thiol dramatically destabilizes the unmodified DNA by ~ 25 ºC while the incorporation of both the 5' and 3' thiols only destabilizes the unmodified DNA by ~ 10 ºC. The added thermal stability observed for

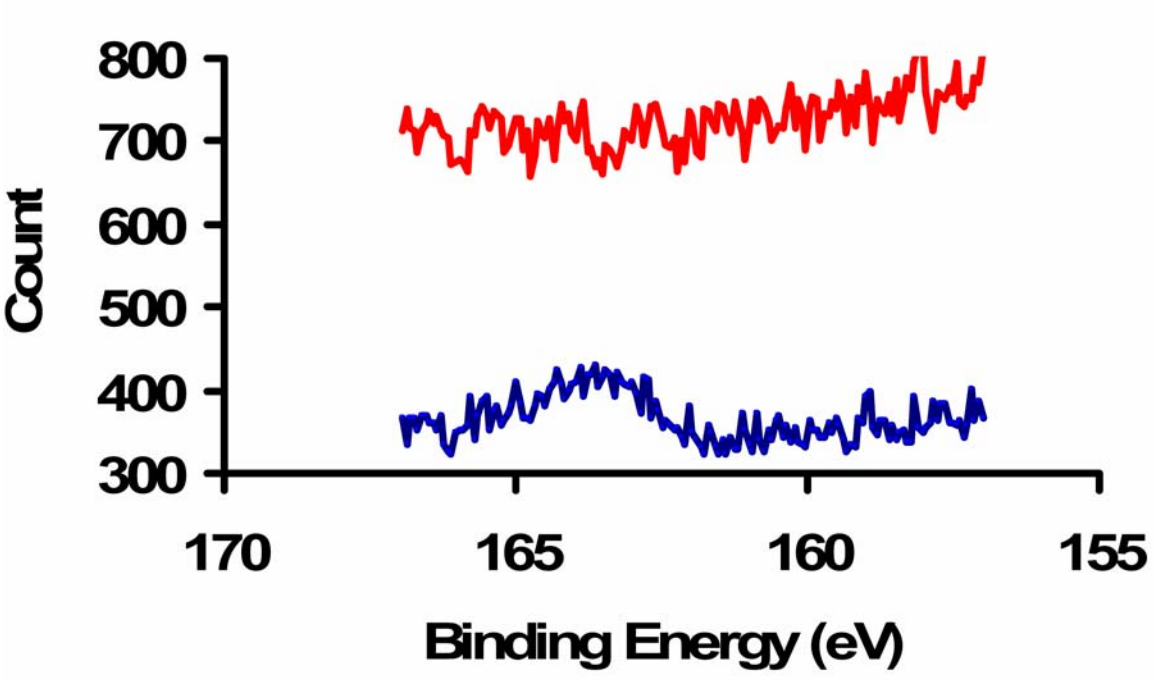

Figure 4.2: XPS spectra of HOPG modified with pyrenated DNA with (blue) and without (red) disulfides incorporated within the sugar phosphate backbone. Note the presence of a small signal at ~ 164 eV for the thiol-modified DNA.

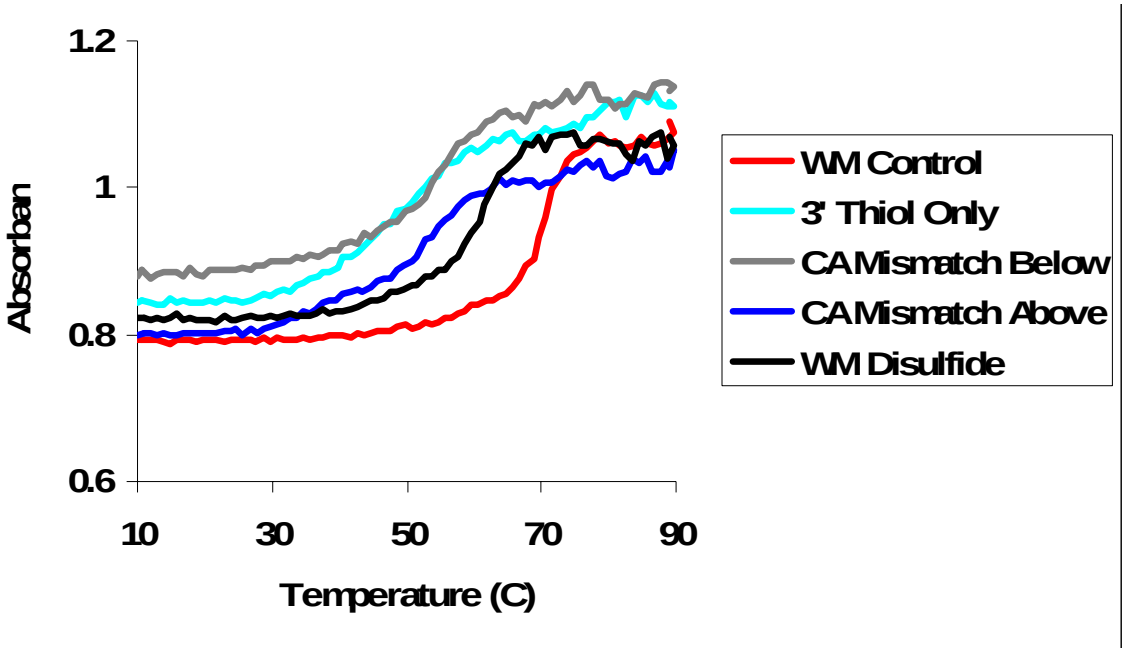

Figure 4.3: Melting temperatures of DNA duplexes as monitored by a change in absorbance at 260 nm. (Red) Well-matched DNA featuring no thiols. (Black) Well-matched DNA featuring two thiols. (Light Blue) Well-matched DNA featuring only a 3' thiol. (Dark Blue) DNA with a CA mismatch above the disulfide. (Gray) DNA with a CA mismatch below the disulfide. The 24 mer sequence utilized in the course of these experiments was pyrene-$(CH_2)_3$-CONH-$(CH_2)_6$-NHCO-5'-ATG CA***T*** CGA C-*S*-*S*-CA CAG TGC T***G***T CGT-3' plus unmodified complement. The locations of the CA mismatches are in bold italics.

two contiguous thiol modifications provides strong evidence for disulfide bond formation. In the absence of such a covalent bond, the opposite effect would be observed after incorporation of two potentially destabilizing modifications.

4.3.3 Electrochemistry of Disulfides Incorporated in the Phosphate Backbone

The DNA-mediated electrochemical reduction of a disulfide incorporated within the DNA sugar-phosphate backbone is schematically illustrated in Figure 4.1. The corresponding electrochemistry of a well-matched DNA monolayer featuring a disulfide is illustrated in Figure 4.4 by square wave voltammetry (SWV) and Figure 4.5 by cyclic voltammetry (CV). Two signals centered at -160 ± 10 mV and at -290 ± 10 mV versus the normal hydrogen electrode (NHE) are observed. The first peak is electrochemically irreversible, and the second peak is electrochemically reversible. Neither signal is found for monolayers lacking the 3' thiol (Figure 4.4). Furthermore, a plot of peak current as a function of scan rate is linear for the cathodic waves of the reversible signal (Figure 4.5), as expected for a surface bound species (35).

The reaction is mediated by the base pair stack, as evidenced by the effect of base mismatches on the second, reversible peak. For well-matched DNA featuring a disulfide, the reversible electrochemical signal exhibits a peak current of 150 ± 30 nA (Figure 4.4). The incorporation of a CA mismatch below the thiols leads to significant attenuation of the electrochemical signal with a resulting peak current of 4 ± 7 nA. On the other hand, the incorporation of a CA mismatch above the thiols has little effect on the signal with a corresponding peak current of 124 ± 7 nA. It is interesting to note that both sequences which feature the CA mismatch are destabilized relative to the well-matched DNA. Therefore, the dramatic attenuation of the signal observed with the CA mismatch below

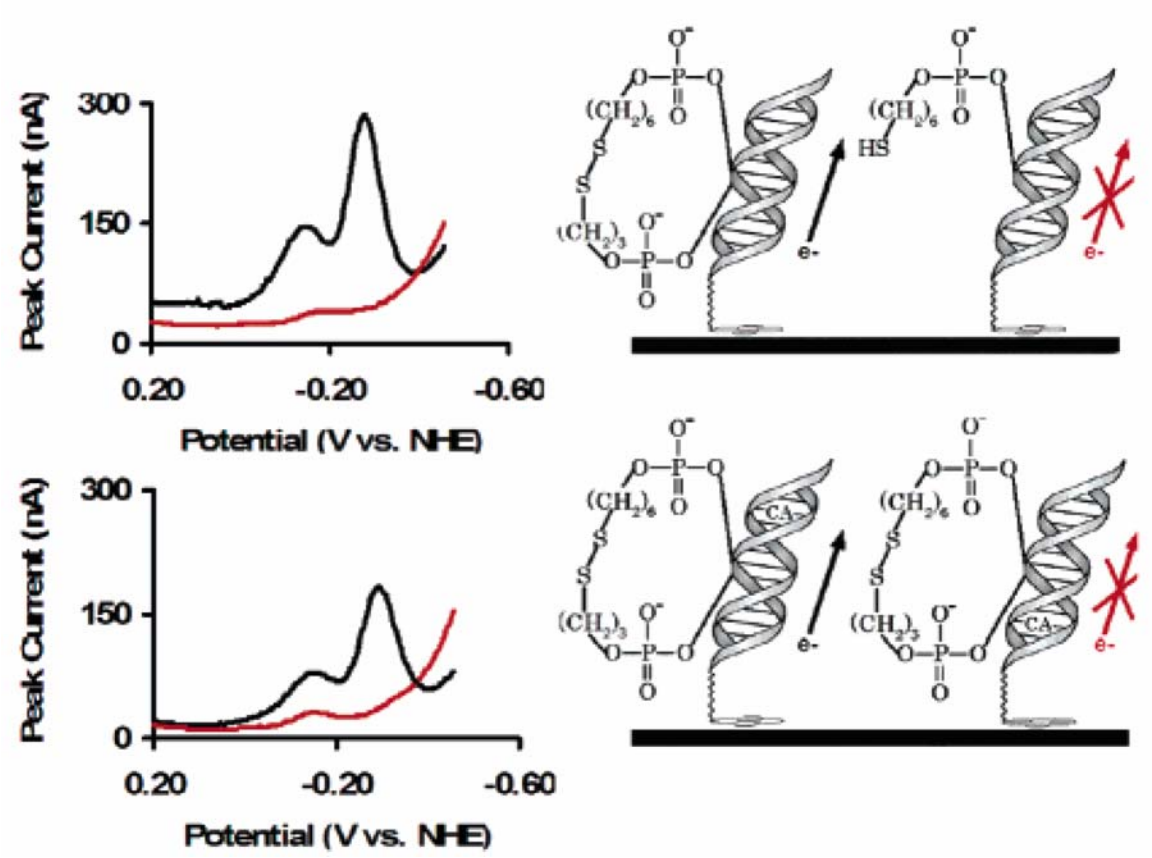

Figure 4.4: SWV at 15 Hz (left) and schematic (right) for various DNA monolayers. Top: Well-matched DNA featuring two thiols (black) and well-matched DNA featuring one thiol (red). Bottom: DNA featuring a CA mismatch above the disulfide (black) and DNA featuring a CA mismatch below the disulfide (red). The 24 mer sequence utilized in the course of these experiments was pyrene-$(CH_2)_3$-CONH-$(CH_2)_6$-NHCO-5'-ATG CA***T*** CGA C-***S***-***S***-CA CAG TGC TGT CGT-3' plus unmodified complement. The locations of the CA mismatches are in bold italics.

A.

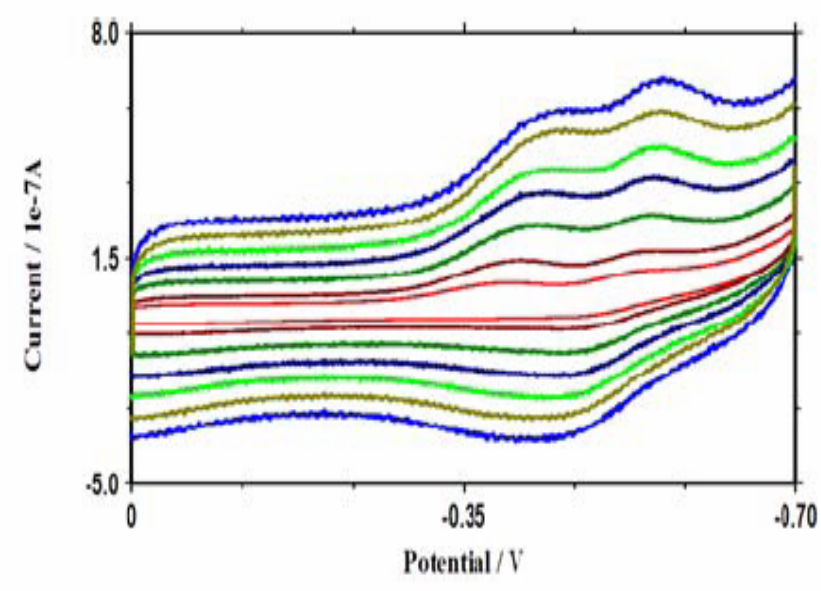

B.

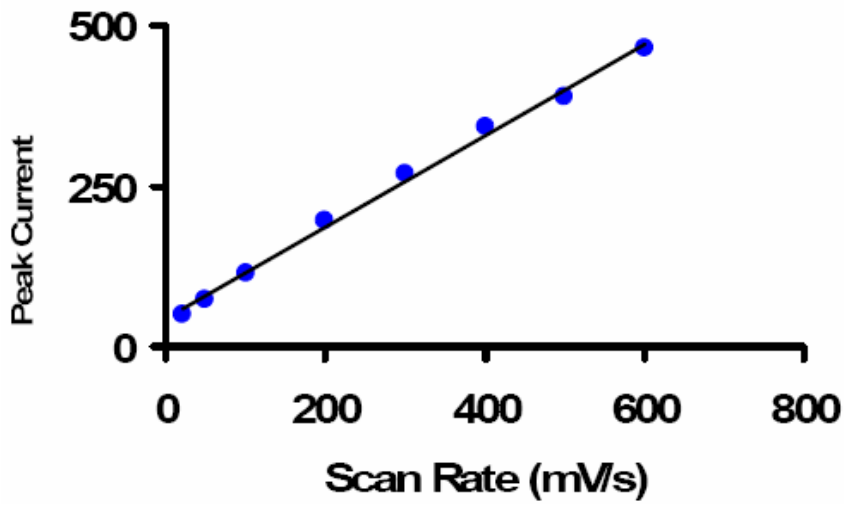

Figure 4.5: A: Cyclic voltammetry at various scan rates of an electrode modified with duplex DNA featuring a disulfide in the sugar phosphate in a pH=7.1 buffer containing 5 mM Na^+ P_i, 50 mM NaCl. B: The corresponding plot of peak current as a function of scan rate for the reversible second wave.

cannot be simply explained by differences in thermal stabilities between DNA with and without a mismatch.

We can interrogate these redox signals further by varying the solution pH (Figure 4.6). Two proton coupled steps are observed electrochemically. These signals are similar to the two separate one-electron reduction steps that have been previously reported for the electrochemistry of the cysteine active site of thioredoxins at similar potentials (36, 37). As the pH, is changed, the amplitude of the reversible signal remains nearly constant, and the midpoint potential of this signal shows a linear pH dependence with a slope of 44 ± 5 mV per pH unit. Although a slope of 59 mV per pH unit is expected for the proton-coupled transfer of one electron, similar nonidealized pH responses have also been observed for DNA polyion films on graphite (38). On the other hand, the amplitude of the irreversible signal is significantly affected by changes in pH. At acidic pH, the irreversible cathodic wave is almost completely suppressed, while, at basic pH, the irreversible cathodic wave is substantially enhanced.

A plausible reaction scheme accounts for these electrochemical data. Although the reduction of a disulfide to two thiols often proceeds through many intermediates, it is a net 2 e^-, 2 H^+ process (39–41). For our system, we can postulate that the addition of the first electron leads to a disulfide radical anion, which we assign to the irreversible peak; at acidic pH, this irreversible reduction is suppressed (42, 43). The reversible addition of two electrons to the disulfide results in disproportionation with concomitant free thiol formation. Thus, the reversible formation of free thiols may be a concerted 2 e^-, 2 H^+ process.

A.

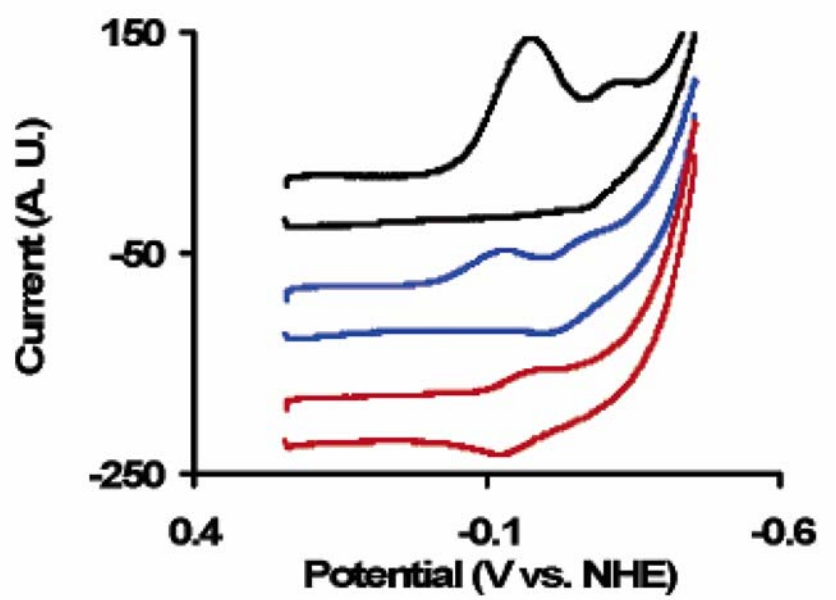

B.

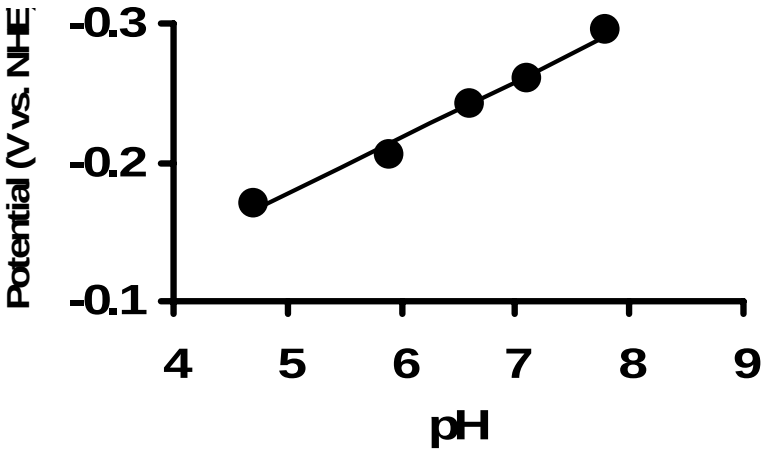

Figure 4.6: (A) Cyclic voltammetry of well-matched DNA featuring a disulfide in 5 mM Na^+ P_i, 50 mM NaCl at a 50 mV/s scan rate. The black, blue, and red traces represent pH 7.8, 6.6, and 4.7, respectively. The blue and red traces have been offset for clarity. (B) The corresponding plot of peak potential as a function of pH.

4.4 Implications

We have therefore shown that DNA-mediated electrochemistry can promote reactions at a distance on the DNA sugar-phosphate backbone. We had earlier seen that breaks in the backbone cause little attenuation in DNA-mediated charge transport through the base stack. We can reconcile these observations by noting relative current densities for DNA-mediated disulfide reduction, 1.8 $\mu A/cm^2$, versus well-stacked intercalator reduction, ~ 80 $\mu A/cm^2$ for daunomycin (27–29). DNA-mediated reactions neighboring but not coupled into the sugar-phosphate backbone are therefore less efficient. Nonetheless, these results expand the reactions that can be achieved through DNA-mediated charge transport chemistry. When one notes that many DNA regulatory proteins utilize disulfide switches in close proximity to the DNA backbone (44–46), these results may be important to consider in a biological context.

REFERENCES

(1) Delaney, S., Barton, J. K. (2003) *J. Org. Chem. 68*, 6475–6483.

(2) O'Neill, M. A., Barton, J. K. (2005) *Charge Transfer in DNA: From Mechanism to Application* (H.-A. Wagenknecht), pp. 27–75, Wiley-VCH, Hoboken.

(3) Hall, D. B., Holmlin, R. E., Barton, J. K. (1996) *Nature 382*, 731–735.

(4) Nunez, M. E., Hall, D. B., Barton, J. K. (1999) *Chem. Biol. 6*, 85–97.

(5) Henderson, P. T., Jones, D., Hampikian, G., Kan, Y., Schuster, G. B. (1999) *Proc. Natl. Acad. Sci. U.S.A. 96*, 8353–8358.

(6) Bhattacharya, P. K., Barton, J. K. (2001) *J. Am. Chem. Soc. 123*, 8649–8656.

(7) Hall, D. B., Barton, J. K. (1997) *J. Am. Chem. Soc. 119*, 5045–5046.

(8) Dandliker, P. J., Holmlin, R. E., Barton, J. K. (1997) *Science 275*, 1465–1468.

(9) Rajski, S. R., Kumar, S., Roberts, R. J., Barton, J. K. (1999) *J. Am. Chem. Soc. 121*, 5615–5616.

(10) Rajski, S. R., Barton, J. K. (2001) *Biochemistry 40*, 5556–5564.

(11) Boon, E. M., Pope, M. A., Williams, S. D., David, S. S., Barton, J. K. (2002) *Biochemistry 41*, 8464–8470.

(12) Meggers, E., Michel-Beyerle, M. E., Giese, B. (1998) *J. Am. Chem. Soc. 120*, 12950–12955.

(13) Lewis, F. D., Liu, X. Y., Liu, J. Q., Miller, S. E., Hayer, R. T., Wasielewski, M. R. (2000) *Nature 406*, 51–53.

(14) Takada, T., Kawai, K., Fujitsuka, M., Majima, T. (2004) *Proc. Natl. Acad. Sci. U.S.A. 101*, 14002–14006.

(15) O'Neill, M. A., Barton, J. K. (2004) *J. Am. Chem. Soc*. *126*, 11471–11483.

(16) Shao, F. W., O' Neill, M. A., Barton, J. K. (2004) *Proc. Natl. Acad. Sci. U.S.A. 101*, 17914–17919.

(17) Vicic, D. A., Odom, D. T., Nunez, M. E., Gianolio, D. A., McLaughlin, L. W., Barton, J. K. (2000) *J. Am. Chem. Soc. 122*, 8603–8611.

(18) Giese, B., Carl, B., Carl, T., Carell, T., Behrens, C., Hennecke, U., Schiemann, O., Feresin, E. (2004) *Angew. Chem. Int. Ed*. 2004, *43*, 1848–1851.

(19) Ito, T., Rokita, S. E. (2004) *Angew. Chem. Int. Ed*. *43*, 1839–1842.

(20) Wagner, C., Wagenknecht, H.-A. (2005) *Chem.-Eur. J. 11,* 1871–1876.

(21) Kaden, P., Mayer-Enthart, E., Trifonov, A., Fiebig, T., Wagenknecht, H.-A. (2005) *Angew. Chem. Int. Ed*. *44*, 1636–1639.

(22) Manetto, A., Breeger, S., Chatgilialoglu, C., Carell, T. (2006) *Angew. Chem., Int. Ed*. *45*, 318–321.

(23) Takada, T., Barton, J. K. (2005) *J. Am. Chem. Soc*. *127*, 12204–12205.

(24) Kelley, S. O., Boon, E. M., Barton, J. K., Jackson, N. M., Hill, M. G. (1999) *Nucl. Acids Res*. *27*, 4830–4837.

(25) Boon, E. M., Ceres, D. M., Drummond, T. G., Hill, M. G., Barton, J. K. (2000) *Nat. Biotechnol*. *18*, 1096–1100.

(26) Boon, E. M., Salas, J. E., Barton, J. K. (2002) *Nat. Biotechnol*. *20*, 282–286.

(27) Kelley, S. O., Jackson, N. M., Hill, M. G., Barton, J. K. (1999) *Angew. Chem. Int. Ed. 38*, 941–945.

(28) Drummond, T. G., Hill, M. G., Barton, J. K. (2004) *J. Am. Chem. Soc*. *126*, 15010–15011.

(29) Liu, T., Barton, J. K. (2005) *J. Am. Chem. Soc. 127*, 10160–10161.

(30) Gorodetsky, A. A., Barton, J. K. (2006) *Langmuir 22*, 7917–7922.

(31) Love, J. C., Estroff, L. A., Kriebel, J. K., Nuzzo, R. G., Whitesides, G. M. (2005) *Chem. Rev*. *105*, 1103–1170.

(32) Kelley, S. O., Barton, J. K., Jackson, N. M., Hill, M. G. (1997) *Bioconjugate Chem*. *8*, 31–37.

(33) Bansal, A., Li, X. L., Yi, S. I., Weinberg, W. H., Lewis, N. S. (2001) *J. Phys. Chem. B 105*, 10266–10277.

(34) Johnson, P. A., Levicky, R. (2004) *Langmuir 20*, 9621–9627.

(35) Bard, A. J., Faulkner, L. R. (2001) *Electrochemical Methods*, *2nd ed.*, John Wiley & Sons: New York.

(36) Salamon, Z., Tollin, G., Hirasawa, M., Gardet-Salvi, L., Stritt-Etter, A.-L., Knaff, D. B., Schurmann, P. (1995) *Biochim. Biophys. Acta 1230*, 114–118.

(37) Johnson, D. L., Polyak, S. W., Wallace, J. C., Martin, L. L. (2004) *Lett. Pept. Sci*. *10*, 495–500.

(38) Munge, B., Estavillo, C., Schenkman, J. B., Rusling, J. F. (2003) *ChemBioChem 4*, 82–89.

(39) Gilbert, H. F. (1995) *Methods Enzymol. 251*, 8–28.

(40) Schoenich, C. (1995) *Methods Enzymol. 251*, 45–55.

(41) Houee-Levin, C. (2002) *Methods Enzymol. 353*, 35–44.

(42) Goebl, M., Bonifacic, M., Asmus, K.-D. (1984) *J. Am. Chem. Soc. 106*, 5984–5988.

(43) Lmoumene, C., Conte, D., Jacquot, J.-P., Houee-Levin, C. (2000) *Biochemistry 39*, 9295–9301.

(44) Das, K. C., White, C. W. (2002) *Proc. Natl. Acad. Sci. U.S.A. 99*, 9617–9618.

(45) Sevier, C. S., Kaiser, C. A. (2002) *Nat. Rev. Mol. Cell Biol. 3*, 836–847

(46) Tooze, J., Branden, C. (1998) *Introduction to Protein Structure*, *2nd ed.,* Garland Publishing: New York.